Journal of the European Ceramic Society 7 (1991) 385–396

Microstructural Characterization of Aluminum Titanate-based Composite Materials

Hans Wohlfromm,[a,b] Thierry Epicier,[b,c] José S. Moya,[a,*]
Pilar Pena[a] & Gareth Thomas[b]

[a] Instituto de Cerámica y Vidrio, C.S.I.C., 28500 Arganda del Rey, Madrid, Spain
[b] National Center for Electron Microscopy, Materials and Chemical Science Division, 1 Cyclotron Road, Berkeley, CA 94720, USA
[c] Institut National des Sciences Appliquées, GEMPPM, u.a. CNRS 341, 69621 Villeurbanne, France

(Received 15 November 1990; revised version received 28 January 1991; accepted 30 January 1991)

Abstract

An extensive microstructural characterization of Al_2TiO_5, MgO-stabilized Al_2TiO_5, and Al_2TiO_5/mullite/ZrO_2 composites, stabilized and unstabilized, was performed using scanning electron and transmission electron microscopy. Complete disorder was found by high-resolution electron microscopy in the cationic sublattice of Al_2TiO_5, even in the presence of Mg. An analysis of Burgers vectors of dislocations in Al_2TiO_5 is presented. EDXS analysis of the aluminum titanate bulk in MgO-stabilized samples gave direct evidence for the formation of solid solutions of the type $Al_{2(1-x)}Mg_xTi_{1+x}O_5$ with improved thermal stability. TEM revealed the presence of a glassy phase in all samples. EDXS analysis of the glassy phase showed repartition of Mg between the Al_2TiO_5 matrix and the glass, reducing the effectiveness of the stabilizing agent MgO. Intergranular ZrO_2 inclusions were found to interact with microcracks, yielding improved mechanical strength of the composite samples.

Die Gefüge von Al_2TiO_5, MgO-stabilisierten Al_2TiO_5 und stabilisierten sowie unstabilisierten Al_2TiO_5/Mullit/ZrO_2-Verbundwerkstoffen wurden mittels Raster-und Transmissionselektronenmikroskopie ausgiebig untersucht. Hochauflösende Elektronenmikroskopie konnte zeigen, daß, selbst in der Gegenwart von Mg, das Kationengitter des Al_2TiO_5 völlig ungeordnet ist. Weiterhin wurde eine Burgersvektoranalyse von Versetzungen in Al_2TiO_5 durchgeführt. Eine EDX-Analyse der Al_2TiO_5-Matrix der mit MgO-stabilisierten Proben konnte die Existenz von $Al_{2(1-x)}Mg_xTi_{1+x}O_5$-Mischkristallen mit verbesserter thermischer Stabilität nachweisen. Glasige Korngrenzenphasen konnten mittels TEM in allen Proben nachgewiesen werden. EDX-Analysen dieser Glasphasen konnten zeigen, daß Mg sowohl in der Al_2TiO_5-Matrix wie auch in der Glasphase vorliegt. Dies reduziert die Wirksamkeit von MgO als Stabilisator. Eine Wechselwirkung zwischen im Gefüge verteilten ZrO_2-Teilchen und auftretenden Mikrorissen konnte nachgewiesen werden und wird für die verbesserte Festigkeit des Verbundwerkstoffs verantwortlich gemacht.

On a étudié de manière approfondie, par microscopies à balayage et à transmission, les microstructures des matériaux suivants: Al_2TiO_5, Al_2TiO_5 stabilisé par MgO et composites Al_2TiO_5/mullite/ZrO_2 stabilisés ou non. La microscopie électronique à haute résolution a révélé un désordre complet dans le sous-réseau cationique de Al_2TiO_5, et ceci même en présence de Mg. On présente une analyse des vecteurs de Burgers des dislocations de Al_2TiO_5. L'analyse EDXS du titanate d'aluminium dans les échantillons stabilisés par MgO prouve la formation de solutions solides du type $Al_{2(1-x)}Mg_xTi_{1+x}O_5$ qui possèdent une stabilité thermique améliorée. La microscopie à transmission a permis de montrer que tous les échantillons présentaient une phase vitreuse. Par analyse EDXS de la phase vitreuse, on a mis en évidence que du Mg était réparti entre la matrice Al_2TiO_5 et le verre, réduisant ainsi l'efficacité du stabilisant MgO. Les inclusions intergranulaires de ZrO_2 interagissent avec les microfissures, conduisant ainsi à une résistance mécanique améliorée des échantillons composites.

* To whom all correspondence should be addressed.

Journal of the European Ceramic Society 0955-2219/91/$3.50

Table 1. Characteristics of reaction-sintered composites and monolithic ceramics based on aluminum titanate[4]

	Code			
	AT100[a]	*AT80*[a]	*MAT100*	*MAT80*
Phase composition	Al_2TiO_5	Al_2TiO_5/mullite/ZrO_2	$(Al_2TiO_5)_{ss}$[b]	$(Al_2TiO_5)_{ss}$/mullite/ZrO_2[b]
Firing temperature, °C	1 500	1 500	1 450	1 450
Bulk density, g/cm^3	3·57	3·63	3·62	3·60
Strength, (MPa)[c]	7·5 ± 0·5	42 ± 2	15·8 ± 0·7	66 ± 3
CTE, 10^{-6} K^{-1}[d]	−0·4	+0·8	−1·0	−0·2
Thermal stability, Φ, 24 h/200 h at 1150°C[e]	0/0	0/0	1/0·93	1/0·74

[a] 100 and 80 refer to an Al_2TiO_5 content of 100 and 80 respectively.
[b] ss indicates stabilization with 2 wt% MgO.
[c] Three-point bending strength.
[d] Coefficient of linear thermal expansion between 20 and 1000°C.
[e] Φ = weight fraction $Al_2TiO_5/(Al_2TiO_5 + TiO_2)$.

1 Introduction

Aluminum titanate is, owing to its low thermal conductivity, low thermal expansion and excellent thermal shock resistance, an interesting candidate for many structural applications, in particular, for the thermal insulation of engine components.[1] However, its poor mechanical properties[2] and thermal instability below 1280°C[3] constitute a serious limitation of its practical utility. Therefore, research efforts concerned with aluminum titanate are, above all, focusing on the improvement of its mechanical properties and thermal stability.

In a recent investigation,[4] it has been shown that aluminum titanate composites with improved properties can be obtained by reaction sintering of $Al_2O_3/TiO_2/ZrSiO_4$ and $Al_2O_3/TiO_2/ZrSiO_4/MgO$ mixtures according to the equations:

$$20\,Al_2O_3 + 17\,TiO_2 + 12\,ZrSiO_4 \rightarrow 17\,Al_2TiO_5 + Al_6Si_2O_{13} + ZrO_2 \quad (1)$$

$$18{\cdot}3\,Al_2O_3 + 18{\cdot}7\,TiO_2 + 2\,ZrSiO_4 + 1{\cdot}7\,MgO \rightarrow 17\,Al_{1{\cdot}8}Mg_{0{\cdot}1}Ti_{1{\cdot}1}O_5 + Al_6Si_2O_{13} + 2\,ZrO_2 \quad (2)$$

The most important characteristics of these composites together with the corresponding monophasic ceramic are given in Table 1. A detailed description of the processing procedure is given elsewhere.[4] From Table 1 it is evident that the introduction of dispersed mullite and ZrO_2 into an Al_2TiO_5 matrix improves the bending strength of the composite notably. Addition of MgO not only yields a slight additional increase in strength but also stabilizes Al_2TiO_5 both in the monophasic specimen (MAT100) and in the composite (MAT80). These improvements have been achieved without deteriorating the thermal expansion characteristics of the composite. Table 2 summarizes the chemical analysis of the studied compounds.

The goal of the present work is to provide a better understanding of the effect of both a solid solution additive (MgO) and second phases (mullite, ZrO_2) on the properties of aluminum titanate-based materials by means of an extensive microstructural characterization through scanning and transmission electron microscopy.

2 Experimental Procedure

Scanning electron microscopy (SEM) was conducted on diamond-polished and chemically etched (15% HF) cross-sections on a Zeiss DSM 950 machine using the secondary electron mode.

Thin foils for transmission electron microscopy (TEM) observations were obtained following a classical procedure of grinding and ion thinning (5 kV Ar ions, incident angle 20°) of diamond saw

Table 2. Chemical analysis after attrition milling (wt%)

	AT100	*AT80*	*MAT100*	*MAT80*
Al_2O_3	55·0	52·8	48·4	47·2
TiO_2	43·4	36·4	47·0	40·2
ZrO_2	0·28	6·33	0·34	6·19
SiO_2	0·48	3·50	0·48	3·22
MgO	0·067	0·067	1·97	1·56
CaO	0·061	0·048	0·098	0·062
Fe_2O_3	0·018	0·030	0·040	0·033
Na_2O	0·07	0·085	0·085	0·085
K_2O	0·01	0·024	0·024	0·024
P_2O_5[a]	0·1	0·1	0·1	0·1
I.L.	0·7	0·8	1·2	1·1

[a] Low precision.

cuts. Different microscopes were used for the various aspects of a general microstructural characterization:

(i) High-resolution electron microscopy (HREM) observations were conducted on the Jeol atomic resolution microscope (ARM) at the National Center of Electron Microscopy, Lawrence Berkeley Laboratory, Berkeley, CA); this instrument offers a unique combination of resolution (about 0·16 nm at 800 kV[5]) and tilting (double tilt 'top entry' stage $\pm 40°$) performances. The multislice-based simulation programs NECMSS[6] were used in order to confirm experimental HR micrographs.

(ii) Conventional TEM work was done on Philips 400 (100 kV) and Jeol 200 CX (200 kV) microscopes.

(iii) Chemical micro-analyses were performed on a dedicated analytical electron microscope (AEM JEOL 200 CX) with an energy dispersive X-ray spectrometry (EDXS) Kevex 800 analyst, mounted with an ultra-thin window detector (allowing light elements to be analyzed). Occasionally analyses were also made on the Philips 400 and Jeol 200 CX (Centre d'Etudes et de Caracterisation Microestructurales, INSA, Villeurbanne, France), equipped with similar systems (but with conventional thin window detectors).

3 Results

3.1 Crystallographic aspects

3.1.1 HREM structural study of Al_2TiO_5

The crystal structure of Al_2TiO_5 has previously been determined by X-ray refinements.[7,8] This material is isomorphous with pseudobrookite, crystallizing in orthorhombic space group *Cmcm* with cell dimensions $a = 0{\cdot}359$, $b = 0{\cdot}943$ and $c = 0{\cdot}965$ at room temperature. An HREM investigation, reported in detail elsewhere[9] confirms a previous result from Morosin & Lynch,[8] i.e. complete disorder in the Al and Ti metal sites for pure Al_2TiO_5 (AT100, see Fig. 1). A similar conclusion can be drawn from the examination of the MgO-stabilized compounds;[9] thus, Mg does not modify the cationic distribution within the aluminum titanate sublattice.

3.1.2 Dislocation analysis

CTEM observations reveal a noticeable dislocation density in the four compounds listed in Table 1. Although their general microstructure is not identical from AT100 to MAT80 (see Fig. 2), dislocations appear to have the same crystallographic characteristics, i.e. Burgers vector **b** and the plane in which the defect is lying, $P = (\mathbf{b}, \mathbf{u})$, where **u** is the line direction.

Figure 2(a) and (b) illustrate a '**g.b**' analysis which has allowed the Burgers vector to be identified as being colinear to [100] and $[1 \pm 10]$. Lattice imaging has made it possible to determine directly the length of the Burgers vector of the latter type as being $\frac{1}{2}[110]$;[10] no evidence was found for any dissociation of the perfect dislocation. Consistently, nodes in Fig. 2(a) and (b) are due to the dislocation reaction:

$$\tfrac{1}{2}[110] + \tfrac{1}{2}[1\bar{1}0] \rightarrow [100]$$

A stereographic analysis indicates that the most frequently found P planes are (01 ± 1) and (001) for **b** equal to $\pm[100]$ and $\pm\frac{1}{2}[1 \pm 10]$ respectively.

The analysis of Burgers vectors and habit planes is consistent with elementary crystallographic considerations: [100]- and $\frac{1}{2}[110]$-type translation vectors are the shortest ones (0·36 and 0·53 nm respectively), and (011) and (001) are two of the densest planes; these planes are then probably easy glide planes. However, it appears that many dislocations are lying in exotic planes; this indicates that complex glide and climb mechanisms occur, as suggested by the tangled and polygonalized microstructures revealed in Figure 2(c) and (d).

3.2 General microstructure

Representative SEM micrographs of the compounds studied are shown in Fig. 3. All samples are displaying some residual porosity consisting in both large pores at grain boundaries and triple points and small ones inside the grains.

Small quantities of glassy phase, attacked and partially removed by HF, can be found in the composite samples (AT80, MAT80). This glassy phase is located mainly at triple points, but also some of the grain boundaries appear to contain glass. However, after chemical etching, it is quite difficult to discern glassy phases from microcracked grain boundaries on SEM micrographs. The chemical composition of the glass will be discussed later (Section 3.5).

Grain size is of the same order of magnitude in all samples, although a smaller grain size could be expected in the composite. A possible explanation for this finding is that the grain growth inhibiting effect by dispersed ZrO_2 and mullite is counterbalanced by a higher amount of the in part transient liquid phase[4] which favors grain growth. However,

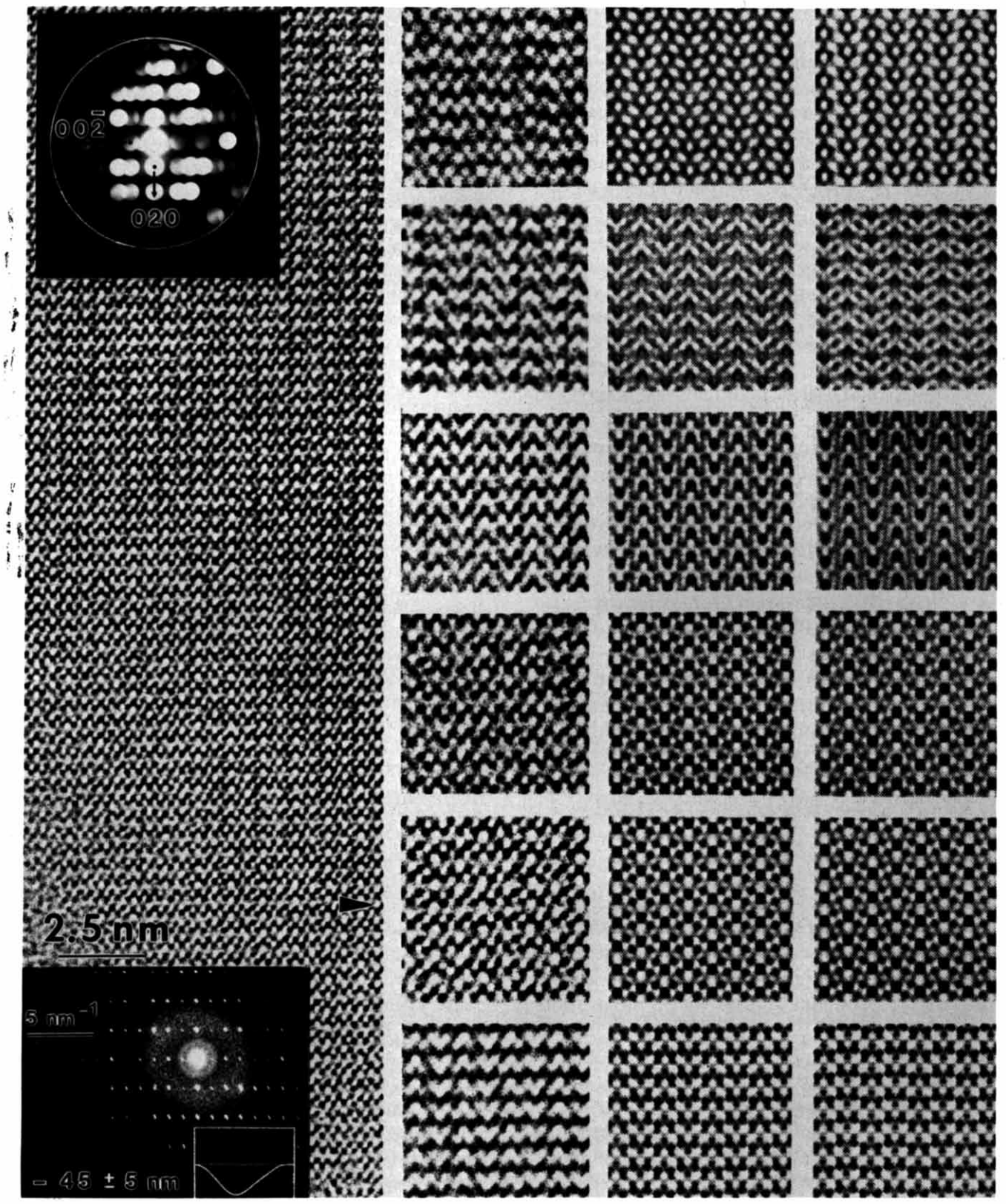

Fig. 1. HREM analysis of AT100 ([100] projection). The matrix of images shows a set of micrographs (b) from the same region (a) taken at various defocus values (images at +15 and −40 nm reveal cation columns as bright and dark spots respectively). Columns (c) and (d) show simulated images calculated from the disordered and ordered models for Al_2TiO_5 at a thickness of 4 nm (see details in Ref. 9).

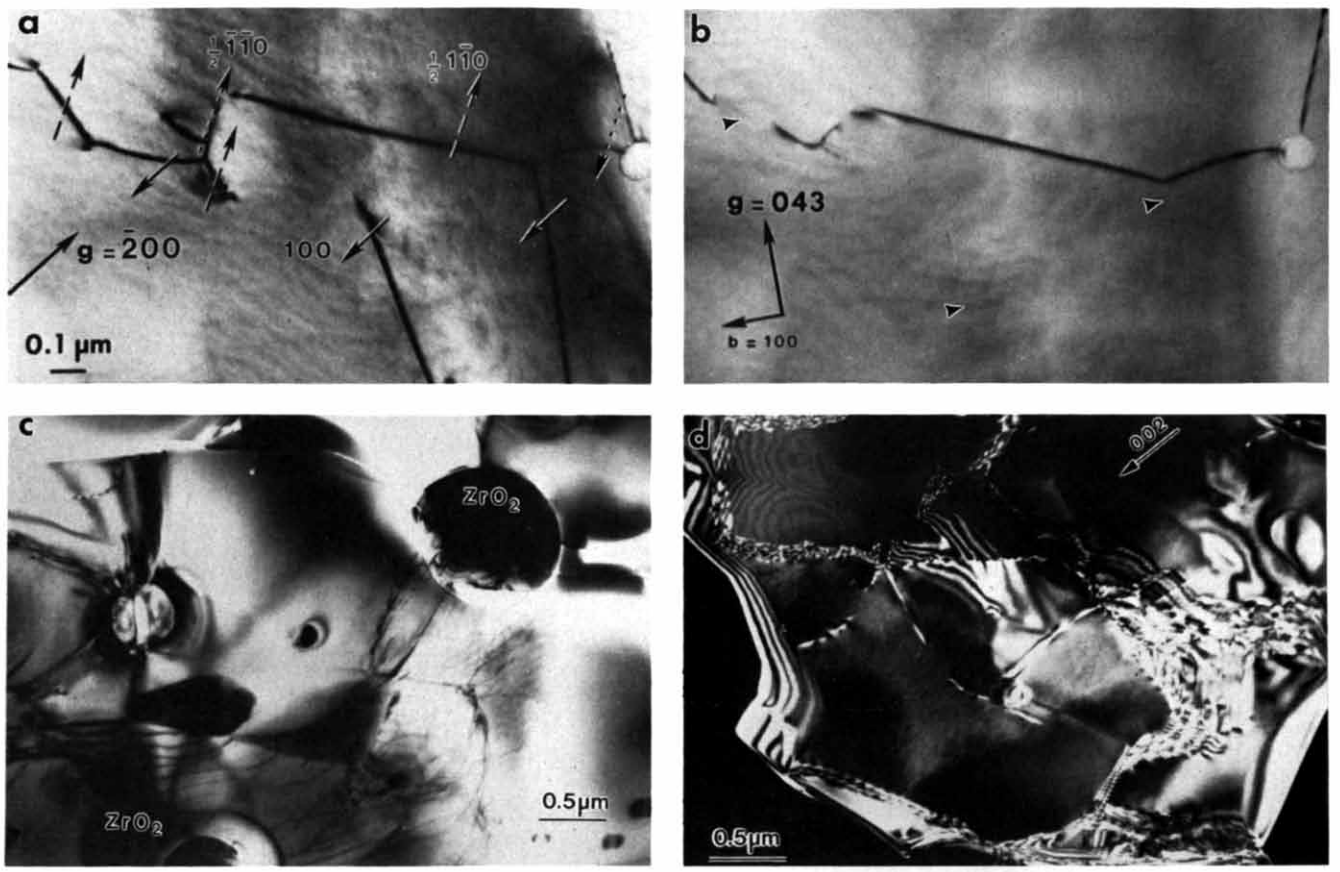

Fig. 2. Dislocation structure in Al_2TiO_5 composites: (a) and (b) two-beam bright field (BF) micrographs showing the same dislocation array in AT100; (c) high density of defects in AT80 (BF image); (d) subgrain boundaries in MAT80 (dark field (DF) image).

there is a remarkable difference in grain morphology. In the AT series (i.e. without MgO) the Al_2TiO_5 grains are almost equiaxed, e.g. in AT100 of aspect ratio = $1{\cdot}4 \pm 0{\cdot}5$, whereas in the MAT series (with the addition of MgO) Al_2TiO_5 grains are of a longish, needle-like shape, e.g. in MAT100 of aspect ratio = $2{\cdot}1 \pm 1{\cdot}1$.

In AT80 and MAT80, ZrO_2 and mullite are found as second phases (Fig. 3(b) and (d)). Since the weak Al_2TiO_5 matrix can not retain tetragonal ZrO_2, which is formed through decomposition of $ZrSiO_4$ in presence of Al_2O_3 (see eqns (1) and (2)), in both cases monoclinic ZrO_2 is present at room temperature, as confirmed by X-ray powder diffraction. Almost spherical ZrO_2 particles, $\leq 3\ \mu m$, are located both at triple points or grain boundaries and, to some extent, inside the grains. The mullite particles are much coarser and of irregular shape in both composites. In AT80, these particles, with a size greater than ZrO_2 but smaller than Al_2TiO_5, are located above all at triple points. In MAT80, the mullite grains are much larger, as large as several Al_2TiO_5 grains, and display an elongated shape.

No specific additional information was obtained through TEM observations about grain size and morphology; however, new features were identified about intra- and intergranular structures, as will be seen in Sections 3.3–3.5.

3.3 Microcracking

The cracking of grain boundary facets is a well-known phenomenon in brittle polycrystalline materials showing anisotropic thermal expansion behavior. For ceramics it is widely recognized that there is a critical grain size for microcracking which is an inverse function of the anisotropy in thermal expansion.[11] Since anisotropy is particularly high in aluminum titanate ($\Delta\alpha_{max} = 23 \times 10^{-6}\,K^{-1}$),[12] the critical grain size is quite small for this material; 1–2 μm[13] and 2·5 μm[14] have been reported in the literature. These microcracks can exert a tremendous effect on properties of aluminum titanate-based ceramics such as elastic modulus, mechanical strength, thermal conductivity, thermal expansion and thermal ·shock resistance.[15–17] From these considerations it is clear that direct characterization of microcracks by SEM and TEM is an important concern of any microstructural study on this material.

During the TEM study of the previously described samples, an appreciable amount of microcracks was detected. However, the high microcrack

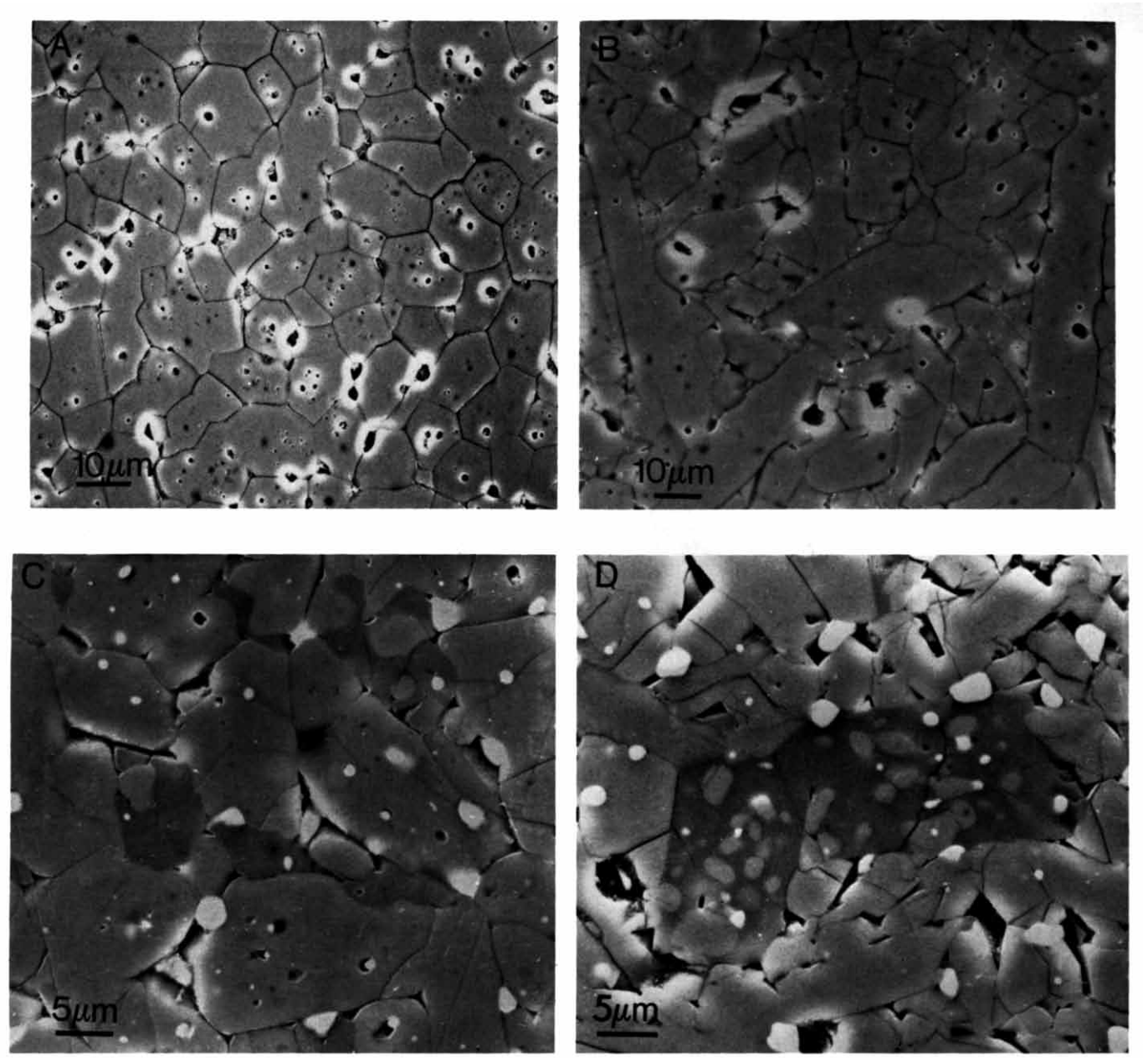

Fig. 3. General microstructure of (A) AT100, (B) MAT100, (C) AT80, (D) MAT80 as observed by SEM on polished and chemically etched cross-sections.

density made the specimen preparation very difficult and, since heavily microcracked areas usually break out during or at the end of the thinning procedure, made it impossible to obtain quantitative information about the microcrack density.

Figure 4 shows typical microcrack configurations of a monophasic (MAT100) and a composite sample (MAT80). Generally, a microcrack extension of more than one grain size was found, but crack length appeared to be shorter in the composites than in the monophasic samples. Figure 4 further demonstrates relatively high crack opening of up to some tenths of a micron. Interaction of the microcracks with the ZrO_2 particles will be discussed.

3.4 Unreacted particles

In the TEM study, an appreciable amount of Al_2TiO_5 grains were found containing a high density of obviously unreacted submicron particles. Typical examples are shown in Fig. 5. Note that most of these particles are associated with dislocations that might have been produced in order to relieve the mechanical stresses exerted from the inclusions on the surrounding Al_2TiO_5 particles, due to differential thermal expansion. EDXS analysis revealed these inclusions to be predominantly Al_2O_3. The existence of excess Al_2O_3 could be explained also from the presence of a small amount of Ti^{3+} in Al_2TiO_5, equivalent to a solid solution of

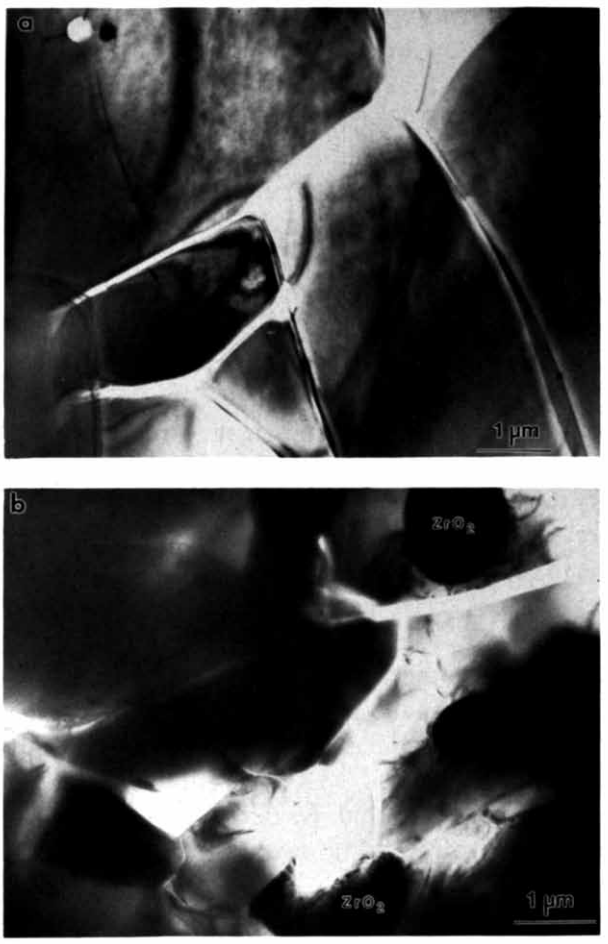

Fig. 4. TEM micrographs showing microcracking in (a) MAT100 and (b) MAT80.

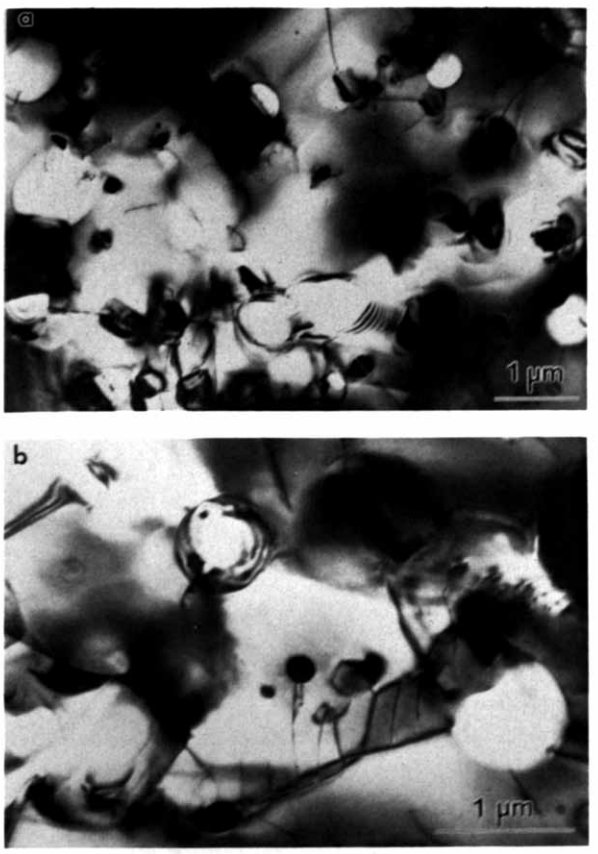

Fig. 5. Occasional evidence (TEM) for a high density of unreacted intragranular particles in (a) AT100 and (b) MAT80.

the type $\{(1-x)Al_2TiO_5 . xTi_3O_5\}$ which would produce exsolution of Al_2O_3. The presence of a small amount of Ti^{3+} in Al_2TiO_5 sintered in air has been proved by NIR/UV–visible spectroscopy (Wohlfromm, H., Durán, A. & Pena, P., unpublished). On the other hand, these inclusions can be addressed as particles which did not react to form Al_2TiO_5 because of local inhomogeneity, then got trapped by rapidly growing Al_2TiO_5 grains and would need longer treatments at temperatures above 1300°C to reach equilibrium, since diffusion through aluminum titanate is rather slow.[18] The fact that above all Al_2O_3 inclusions have been found might be considered a problem of selecting too few grains for analysis.

The possibility can not be ruled out that the aforementioned intragranular porosity is stemming from unreacted particles which have been pulled out during polishing.

It is noteworthy that Al_2O_3 and TiO_2 inclusions represent nucleation centers for the decomposition of Al_2TiO_5 and therefore could notably influence on the thermal stability of aluminum titanate. In fact, for the composites studied in the present work, indication was found that decomposition starts inside the Al_2TiO_5 grains[4] and not at the grain boundaries as reported elsewhere.[19]

3.5 Glassy phase

The existence of a glassy phase in the polyphasic samples AT80 and MAT80 was evident even in SEM micrographs (Fig. 3) as described previously. Such glassy phases must not necessarily be due to impurities but could also indicate incomplete reaction between $ZrSiO_4$ and Al_2O_3, namely, ZrO_2 and mullite are formed as products of a multistep process involving basically (a) decomposition of $ZrSiO_4$, yielding ZrO_2 and a transient silica-rich glassy phase and (b) reaction of the glass with Al_2O_3, giving mullite. There was, however, no clear evidence from SEM for the existence of a glassy phase in the monophasic samples. Nevertheless, the diffused dark field technique in the TEM revealed the existence of a glassy phase also in grain boundaries and above all at triple points of AT100 (Fig. 6(a)) and MAT100 (Fig. 6(b)). This glass is not homogeneously distributed. As a result, perfect, microcracked and glassy grain boundaries are found in AT100 and MAT100. Bubbles in this glassy phase (Fig. 6(b))

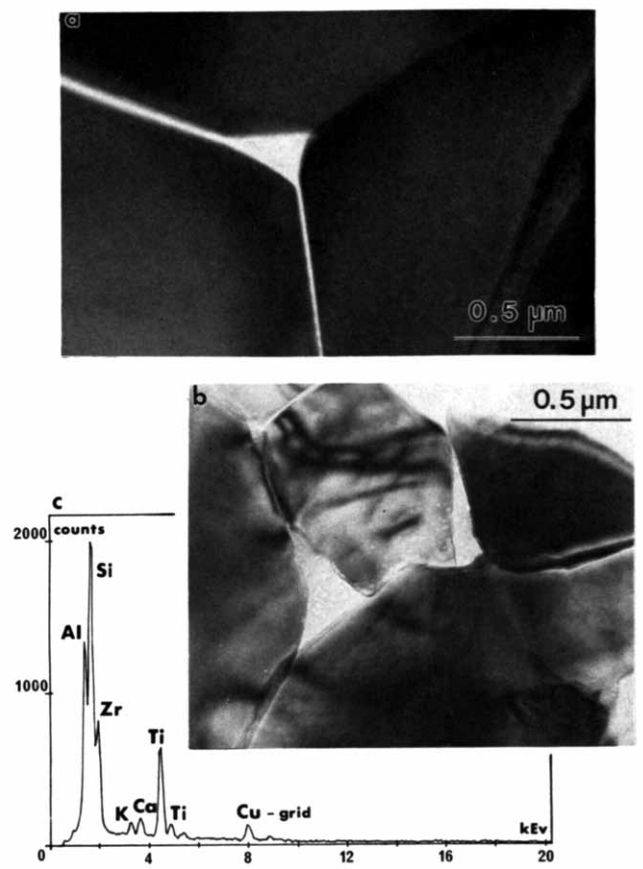

Fig. 6. TEM study of the glassy phase: (a) diffuse dark field image of glassy-grain boundary films and a glassy pocket in AT100; (b) bright field image of large glassy pockets at triple junctions in MAT100; (c) typical EDX spectrum recorded from the glassy pocket in (b).

could be considered as a primary evidence of beginning phase separation or crystallization.

A rough quantitative analysis of the glassy phase in the triple points of the four compounds, such as in Fig. 6(c), obtained by EDXS in the TEM, is reported in Table 3. Al and Ti are not taken into account, since the vicinity of Al_2TiO_5 does not allow a reliable quantitative analysis of these elements. The relatively high content of SiO_2 in MAT100 is surprising but is in accord with the chemical analysis of the overall composition, yielding 0·48 wt% of SiO_2[4] (compare to Table 2). Thus, it might be speculated that the SiO_2 content in Al_2O_3 and/or TiO_2 is in reality higher than that indicated by the supplier (TiO_2, Merck 808 Al_2O_3, Alcoa CT 3000 SG, were used). The fact that Zr is found also in AT100 and MAT100 must be due to contamination through attrition milling with Mg–PSZ balls. Again, this finding is in agreement with chemical analysis, yielding an overall content of 0·28 and 0·34 wt.% for AT100 and MAT100 respectively.[4] Surprisingly, the Zr content of the glassy phase is highest in AT100 and MAT100. To explain this finding it could be speculated that ZrO_2 particles in AT80 and MAT80 act as a sink for the ZrO_2 contamination stemming from milling. Furthermore, no Mg was detected in the glassy phase of AT100 and AT80, whereas Mg is unambiguously present in the glassy phase of MAT compounds. That means there is a distribution of the MgO additive between Al_2TiO_5 and the glassy grain boundary phase, i.e. not all the Mg is really effective in stabilizing aluminum titanate. The fact that the Mg concentration in the glass is higher in MAT80 than in MAT100 is in agreement with the somewhat lower thermal stability of MAT80 (Table 1). The small quantities of Ca and K detected were probably introduced through the raw materials.

Table 3. Main constituents of the glassy phase, determined by EDX (wt.%; indicative values; each column sums to 100% if Al and Ti are taken into account)

	AT100	*AT80*	*MAT100*	*MAT80*
Si	4	27	20	27
Zr	7	2	9	2
Mg	—	—	2	5
Ca	2	1	1	1
K	1	—	1	—

4 Discussion

4.1 Effect of MgO addition

It has been claimed that the stabilizing effect of MgO is due to the formation of a solid solution of the general formula $Al_{2(1-x)}Mg_xTi_{1+x}O_5$, if Al_2O_3 and TiO_2 content are adjusted properly.[20] Ishitsuka *et al.*[20] deduced the existence of this compound from the variation of the lattice parameters with x, measured by X-ray diffraction. In the present study, EDX analysis in the TEM yielded $Al_{2\pm0.2}Ti_{0.9\pm0.1}O_{4.9\pm1}$ (Mg, Zr $\leq$ 0·014 at.%) and $Al_{2\pm0.3}Ti_{1.1\pm0.2}Mg_{0.12\pm0.05}O_{5\pm0.2}$ (Si $\leq$ 0·016 at.%) for AT100 and MAT100 respectively (Fig. 7). That is, direct evidence for the existence of a solid solution corresponding to $x = 0.1$ (2 wt% MgO) is given for the stabilized sample MAT100.

However, it has also been shown above that when Al_2TiO_5 grains are wetted by a glassy grain boundary phase in MAT100 compounds there is a distribution of MgO between Al_2TiO_5 and the glass. That is, not all the MgO will be effective in stabilizing Al_2TiO_5. Consequently, suppressing the glass content by modifying the processing route would probably yield Al_2TiO_5-based compounds with a better thermal stability.

The question arises why a solid solution of MgO

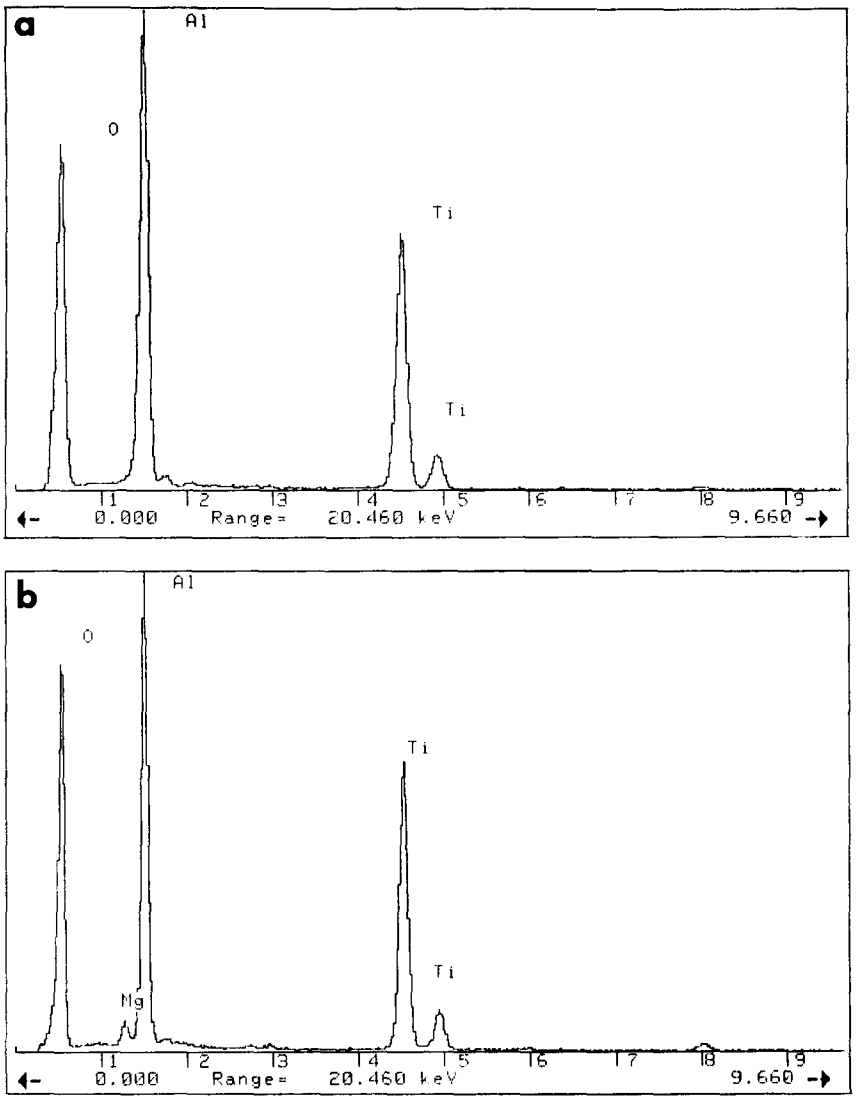

Fig. 7. Typical EDX spectra recorded from the matrix in (a) AT100 and (b) MAT100 using an ultra-thin window detector.

in Al_2TiO_5 leads to stabilization, and the introduction of other oxides such as ZrO_2, which was also reported to form a solid solution in Al_2TiO_5,[14] does not. The explanation usually given in the literature[12] is that Mg^{2+} (ionic radius = 0·66 Å), that substitutes Al^{3+} according to the reaction

$$2Al^{3+} = Mg^{2+} + Ti^{4+}$$

reduces the distortion of oxygen octahedra in the pseudobrookite structure caused by the large difference in ionic radii between Al^{3+} (0·51 Å) and Ti^{4+} (0·68 Å). Analogously, it can be argued that Zr^{4+} (0·79 Å), that substitutes Ti^{4+} according to[21]

$$Ti^{4+} = Zr^{4+}$$

can not stabilize the pseudobrookite structure, since its ionic radius is higher than that of both Al^{3+} and Ti^{4+}.

On the other hand, some authors claim that the thermal instability of Al_2TiO_5 is related to a defect in oxygen stoichiometry.[21,22] Thus, it could be speculated that MgO affects the degree of oxygen deficiency. Although the quantity of oxygen deficiency present in monophasic compounds was directly estimated with the ultra-thin window EDXS equipment of the AEM, the accuracy of these measurements is difficult to define, and the apparent result showing that AT100 would be slightly poorer in oxygen than MAT100 remains questionable; thus, this hypothesis can not be checked through the present investigation.

In addition, from the data reported in this paper it can be concluded that the change in grain morphology observed in presence of MgO is also due to a solid solution effect. It can be assumed that MgO changes the surface energy of certain crystallographic planes in Al_2TiO_5 and therefore favors directional grain growth. However, more TEM work would be necessary to provide information about the nature of these planes. The alternative

hypothesis that directional grain growth was caused by the presence of a glassy phase can be rejected since glass was found in all specimens.

This change in grain morphology is believed to be responsible for the slightly higher bending strength of the specimens containing MgO, since the more needle-like grains in MAT100 and MAT80 are (a) likely to deflect the intergranular propagating cracks and (b) to provide more resistance to crack opening due to frictional interlocking of grains in the crack wake.

4.2 Effect of second phases

The strength of the aluminum titanate-based composites will be determined by propagation and link-up of intergranular microcracks under a mechanical load. The SEM micrographs suggest that small ZrO_2 particles, which are mainly located at triple points and grain boundaries, will be more effective in strengthening aluminum titanate, whereas it might be assumed that the coarse-grained

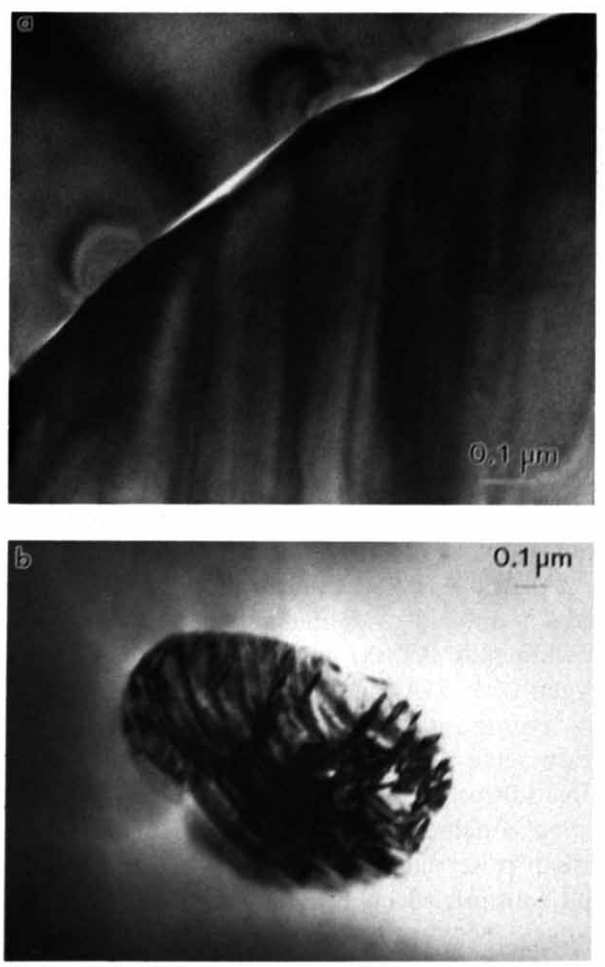

Fig. 8. TEM observation of the ZrO_2/Al_2TiO_5 interface in AT80: (a) evidence for voids and stresses at the interface after the tetragonal–monoclinic transformation during cooling; (b) intragranular ZrO_2 particle.

Fig. 9. TEM evidence for interaction of intergranular microcracks (arrow) with ZrO_2 particles in AT80.

mullite, especially in MAT80, may exert a minor influence.

Since grain size was not affected significantly by introduction of ZrO_2 and mullite the question is which mechanism leads to the pronounced strength increase. Pena *et al.*[23] proposed that the tetragonal to monoclinic transformation of ZrO_2 could produce transgranular microcracks and therefore cause crack propagation to change from intergranular to transgranular, thus leading to a higher strength. However, TEM examination of ZrO_2/Al_2TiO_5 interfaces only yielded occasional evidence for small tangential microcracks at the emergence of twin planes in intergranular monoclinic zirconia particles (see Fig. 8(a)), whereas no grain boundary decohesion was observed in the case of the smaller intragranular particles (Fig. 8(b)).

On the basis of the microstructural observations reported in Figs 4 and 9, an alternative and more likely strengthening model can be proposed. Basically, microcracks in monophasic compounds can propagate relatively easily along the 'weak' grain boundaries, thus leading to a large critical grain size;

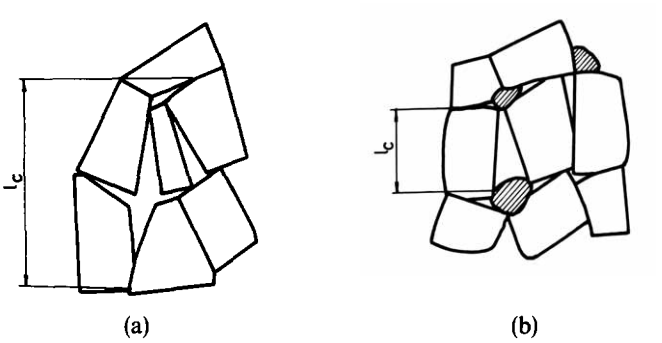

Fig. 10. Schematic illustration of the microcrack network in (a) AT100/MAT100 and (b) AT80/MAT80; note the reduction of continuous cracks (l_c) due to the presence of intergranular ZrO_2 particles (shown shaded in (b)).

in composites such microcracks will lose energy and therefore stop propagation when they encounter ZrO_2 particles with a much higher elastic modulus than the matrix. As a result, flaw size will be smaller in these compounds, thus yielding a higher strength (Fig. 10). This consideration is supported by the fact that strengthening also occurs when other, non-transforming dispersions instead of ZrO_2 are present.[4]

It has been shown also that the presence of second phase particles affects the dislocation microstructure within Al_2TiO_5 grains. Small intergranular Al_2O_3 or TiO_2 particles most probably play a negligible role, since they are impinging individual and rather unorganized dislocations. By contrast, large intergranular ZrO_2 particles modify significantly the density and substructure of dislocations: tangles, networks and rather unorganized dislocations (Fig. 2(c) and 2(d)) being a clear evidence for dislocation activity and probable plastic flow during elaboration (cooling) of the compounds. Further specific deformation studies would, however, be necessary in order to precisely determine the role of the dislocation mechanisms.

5 Conclusions

An extensive microstructure study of Al_2TiO_5, Mg–Al_2TiO_5, as well as the composites Al_2TiO_5/mullite/ZrO_2 and Mg–Al_2TiO_5/mullite/ZrO_2, has been undertaken with the aim to reach a better understanding of the properties of these materials. The following major conclusions can be pointed out:

(1) Direct evidence for the existence of a solid solution of the formula $Al_{2\pm0.3}Ti_{1.1\pm0.2}$-$Mg_{0.12\pm0.05}O_{5\pm0.2}$ was obtained by EDX. The presence of Mg does, however, not effect the complete disorder in the cationic lattice; hence the possibility that order–disorder phenomena are responsible for the stability of aluminum titanate can be excluded.

(2) Silica-rich glassy phases have been found at the grain boundaries and triple points of all compositions. This glassy phase lessens the stabilizing effect of Mg^{2+}, since there is a distribution of Mg^{2+} between the Al_2TiO_5 bulk and the glass.

(3) Dispersed monoclinic ZrO_2 particles, located mainly at triple points and grain boundaries, which interact with microcracks, limit the microcracks to a tolerable length and, thus, improve mechanical properties significantly. In contrast, mullite seems to exert a minor influence on mechanical properties.

(4) Dislocations were found in the Al_2TiO_5 matrix of all compositions; the dislocation density and substructure are modified in the case of interaction with intragranular ZrO_2 inclusions. Further studies are necessary to elucidate the role of these dislocations during elaboration and service of these composites.

Acknowledgements

The authors wish to thank C. Echer for assistance in the AEM analysis. The award of fellowships to H. W. from the Commission of the European Communities and to T.E. from NATO is gratefully acknowledged. Financial support was obtained from CICYT, Spain (project MAT88-0156) and NATO (CRG 890742).

References

1. Stingl, P., Heinrich, J. & Huber, J., Properties and application of aluminum titanate components. In *Proceedings of the 2nd International Symposium on Ceramic Materials and Components for Engines*, Lübeck-Travemünde, FRG, April 1986, ed. W. Bunk & H. Hausner. DKG, Bad Honnef, 1986, pp. 369–80.
2. Heinrich, H., Langer, M. & Siebels, J. E., Experimental results with ceramic components in passenger-car diesel engines. In *Proceedings of the 2nd International Symposium on Ceramic Materials and Components for Engines*, Lübeck-Travemünde, FRG, April 1986, ed. W. Bunk & H. Hausner. DKG, Bad Honnef, 1986, pp. 1155–63.
3. Kato, E., Daimon, K. & Takahashi, J., Decomposition temperature of β-Al_2TiO_5 *J. Am. Ceram. Soc.*, **63**(5–6) (1980) 355–6.
4. Wohlfromm, H., Moya, J. S. & Pena, P., Effect of $ZrSiO_4$ and MgO additions on reaction sintering and properties of Al_2TiO_5-based materials. *J. Mat. Sci.*, **25** (1990) 3753–64.
5. Hetherington, C. D. J., Nelson, E. C., Westmacott, K. H., Gronsky, R. & Thomas, G., *Mat. Res. Soc., Symp. Proc.*, **139** (1989) 277–82.
6. Kilaas, R., In *Proc. 47th Annual Meeting of the Electron Microscopy Society of America*, San Antonio, Texas, 6–11 August 1989, ed. G. W. Bailey. San Francisco Press, San Francisco, 1989, pp. 66–9.
7. Hamelin, M., Structure du composé $TiO_2.Al_2O_3$. Comparison avec la pseudo-brookite. *Bull. Soc. Chim.*, **5** (1958) 1559–66.
8. Morosin, B. & Lynch, R. W., Structure studies on Al_2TiO_5 at room temperature and at 600°C. *Acta Cryst.*, **B28** (1972) 1040–6.
9. Epicier, T. A., Wohlfromm, H., Thomas, G. & Moya, J. S., High resolution electron microscopy study of the cationic disorder in Al_2TiO_5. *J. Mat. Res.*, **6**(1) (1991) 138–45.
10. Epicier, T. A., Wohlfromm, H. & Thomas, G., Dislocation analysis in Al_2TiO_5. In *Proceedings of 47th Annual Meeting*

of the Electron Microscopy Society of America, San Antonio, Texas, 6–11 August 1989, ed. G. W. Bailey. San Francisco Press, San Francisco, 1989, pp. 422–3.
11. Davidge, R. W., Cracking at grain boundaries in polycristalline brittle materials. *Acta Met.*, **29** (1981) 1695–702.
12. Bayer, G., Thermal expansion characteristics and stability of pseudobrookite-type compounds, Me_3O_5. *J. Less-Common Metals*, **24** (1971) 129–38.
13. Cleveland, J. J. & Bradt, R. C., Grain-size/microcracking relations for pseudobrookite oxides. *J. Am. Ceram. Soc.*, **61** (11–12) (1978) 478–81.
14. Ohya, Y., Hamano, K. & Nakagawa, Z., Microstructure and mechanical strength of aluminum titanate ceramics prepared from synthesized powders. *Yogyo-Kyokai-Shi*, **91**(6) (1983) 289–97.
15. Buessem, W. R., Thielke, N. R. & Sarakauskas, R. V., Thermal expansion hysteresis of aluminum titanate. *Ceramic Age*, **60** (1952) 38–40.
16. Bush, A. & Hummel, F. A., High-temperature mechanical properties of ceramic materials: I. Magnesium dititanate. *J. Am. Ceram. Soc.*, **41**(6) (1958) 189–95.
17. Siebeneck, H. J., Cleveland, J. J. Hasselman, D. P. H. & Bradt, R. C., Thermal diffusivities of microcracked polycrystalline ceramics. In *Ceramic Microstructures '76*, ed. R. M. Fulrath & J. A. Pask. Westview Press, Boulder, Colorado, 1976, pp. 753–62.
18. Freudenberg, B. & Mocellin, A., Aluminum titanate formation by solid state reaction of fine Al_2O_3 and TiO_2 powders. *J. Am. Ceram. Soc.*, **70**(1) (1978) 33–8.
19. Locker, R. J., Microstructural characterization of aluminum titanate. Paper No. 36-AC-88P, presented at the 41st Pacific Coast meeting of the American Ceramic Society, San Francisco, CA, October 1988.
20. Ishitsuka, M., Sato, T., Endo, T. & Shimao, M. Y., Synthesis and thermal stability of aluminum titanate solid solutions. *J. Am. Ceram. Soc.*, **70**(2) (1987) 69–71.
21. Hennicke, H. W. & Lingenberg, W., The formation and decomposition of aluminum titanate: II. The decomposition reaction of aluminum titanate. cfi/*Ber. DKG*, **63**(3) (1986) 100–6.
22. Thielke, N. R., Aluminum titanate and related compounds. US Air Force, Air Research and Development Command, WADC, Technical Report No. 53–165, 1953.
23. Pena, P., de Aza, S. & Moya, J. S., Microstructure and mechanical properties of an Al_2TiO_5–Mullite–ZrO_2 Composite obtained by reaction sintering. In *Ceramic Microstructures '86. Role of Interfaces*, ed. J. Pask & A. G. Evans. Plenum Press, NY, London, 1987, pp. 847–57.